Supporting Information

Rose-like, ruthenium-modified cobalt nitride nanoflowers grown *in situ* on an MXene matrix for efficient and stable water electrolysis

Liang Yan, [a,#,*] and Bing Zhang[b,#]

[a] School of Chemistry and Materials Engineering, Guangdong Provincial Key Laboratory of Electronic Functional Materials and Devices, Huizhou University, No. 46 Yanda Road, Huizhou, 516007, China.

[b] School of Materials and Energy, Guangdong University of Technology, No. 100 Waihuan Xi Road, Guangzhou Higher Education Mega Center, Guangzhou, 510006, China.

[*] E-mail: yanliang@hzu.edu.cn (L. Yan)

[#]These authors contributed equally to this work.

Experimental section

Materials

Titanium aluminum carbide (Ti_3AlC_2, ≥98%) was purchased from Foshan Xinxi Technology Co., Ltd (Foshan, China). Cobalt (II) nitrate hexahydrate ($Co(NO_3)_2 \cdot 6H_2O$), N-methyl pyrrolidone (NMP), urea (CH_4N_2O) and ethanol (C_2H_5OH, >99.7%) were obtained from Guangzhou Chemical Reagent Factory (Guangzhou, China). Pt/C (20 wt%), RuO_2, $RuCl_3$ and Nafion solution (5 wt%) were purchased from Sigma-Aldrich. Carbon papers (CP) were purchased from Toray

Industries, Inc. (Tokyo, Japan). All chemicals and materials were used as purchased without further purification.

Synthesis of $Ti_3C_2T_x$ MXene nanosheets

The $Ti_3C_2T_x$ MXene was synthesized by etching Al layer from Ti_3AlC_2 with a mixture of LiF and HCl. Specifically, 2.0 g LiF was added to 40 mL of 9.0 M HCl by stirring for several minutes. Subsequently, 1.0 g Ti_3AlC_2 powder was slowly added into the above solution. After etching for 24 h at 35 °C in water bath under magnetic stirring, the multilayer $Ti_3C_2T_x$ MXene was washed and centrifuged with deionized water for several times until the pH of the supernatant was approximately 6. Next, the obtained sediment was dispersed in 200 mL of deionized water and kept under bath sonicated for 1 h under N_2 gas protection. The dark green supernatant containing monolayer or few-layer $Ti_3C_2T_x$ MXene nanosheets was collected by centrifuging for 1 h at 3500 rpm. The obtained $Ti_3C_2T_x$ MXene solution was reserved at 0 °C in the refrigerator followed by freeze-drying before use.

Synthesis of Ru-CoN/$Ti_3C_2T_x$ MXene

The Ru-Co LDH/$Ti_3C_2T_x$ MXene was synthesized through a simple oil bath method by using $Co(NO_3)_2 \cdot 6H_2O$, $RuCl_3$, and $Ti_3C_2T_x$ MXene as the precursors for the in situ growth Ru-Co LDH nanoflowers on the surface of $Ti_3C_2T_x$ MXene. Typically, 0.2 mmol $Co(NO_3)_2 \cdot 6H_2O$, $RuCl_3$ with different contents (0, 0.022, 0.05, and 0.086 mmol $RuCl_3$ match to 0, 10%, 20%, and 30%, respectively), and 2 mmol urea were dissolved in 20 mL of $Ti_3C_2T_x$ MXene/NMP dispersion (3 mg mL^{-1}). The above mentioned solution was then refluxed at 100 °C for 5 h in a three-necked flask under stirring in N_2

flow. The final Ru-Co LDH/Ti$_3$C$_2$T$_x$ MXene was obtained by centrifugation washed using deionized water and ethanol for five times each followed by freeze-drying. Subsequently, the Ru-Co LDH/Ti$_3$C$_2$T$_x$ MXene precursor was placed at the center of a furnace tube and then heated to 380 °C at the rate of 5 °C min^{-1} and maintained at this temperature for 2 h under a flowing NH$_3$ atmosphere. Finally, the resulting product Ru-CoN/Ti$_3$C$_2$T$_x$ MXene was obtained. For comparison, the bare CoN was prepared by similar approach except that pristine Co LDH instead of Co LDH/Ti$_3$C$_2$T$_x$ MXene was used as the precursor.

Materials characterization

The morphology and nanostructure of samples were characterized with field-emission scanning electron microscopy (FESEM, Hitachi SU8220) and transmission electron microscopy (TEM, FEI Talos F200S) coupled with energy dispersive X-ray (EDX) spectroscopy. Powder X-ray diffraction (XRD) patterns were recorded using X-ray diffractometer (D8 Advance, Bruker) with a Cu kα radiation source (λ = 0.1541 nm) at a scan rate of 8° min^{-1}. X-ray photoelectron spectra (XPS) were performed with a Thermo Fischer ESCALAB 250Xi spectrometer with Al kα radiation source. Raman spectrum were recorded on a LabRAM HR Evolution (Horiba Jobin Yvon, France) using 532 nm laser source.

Electrochemical measurements

All electrochemical measurements were carried out at room temperature in a standard three-electrode cell controlled by PGSTAT302N potentiostat/galvanostat (Metrohm Autolab, Netherlands) electrochemical workstation. A graphite rod and a reversible

hydrogen electrode (RHE) and 1.0 M KOH were used as the counter electrode and reference electrode, respectively. A catalyst ink was prepared by ultrasonically dispersed the mixture of 5 mg of the sample, 10 μL of 5 wt% Nafion solution and 990 μL of ethanol for at least 1 h. Then 10 μL of the catalyst ink was carefully deposited on the surface of a glassy carbon (GC) rotating disk electrode (RDE) with a diameter of 5 mm, and dried naturally. Before and during the HER or OER test, freshly prepared 1.0 M KOH solution was bubbled with Ar or O_2 flow, respectively. After twenty CV scans, the linear sweep voltammetry (LSV) was obtained at a rotating rate of 1600 rpm with a scan rate of 5 mV s^{-1}. All polarization curves were corrected with 90% *iR* compensation. The double-layer capacitances (C_{dl}) were determined by CV method in the non-faradaic potential region with scan rates from 10 to 90 mV s^{-1}. Electrochemical impedance spectroscopy (EIS) was tested in a frequency range from 100 kHz to 0.1 Hz by applying an AC voltage of 5 mV amplitude. The stability tests were carried out under constant current densities of -10 or 10 mA cm^{-2} for HER or OER, respectively. For the two-electrode electrolysis, the as-prepared Ru-CoN/Ti$_3$C$_2$T$_x$ MXene was used as both the anode and cathode.

Fabrication of Ru-CoN/Ti$_3$C$_2$T$_x$ MXene/CP, Pt/C/CP, and RuO$_2$/CP electrodes

Ru-CoN/Ti$_3$C$_2$T$_x$ MXene/CP was prepared by drop-casting method. Typically, 2 mg Ru-CoN/Ti$_3$C$_2$T$_x$ MXene was dispersed in 0.99 mL ethanol with 10 μL 5wt% of Nafion solution, and the mixture solution was subsequently ultrasonically at least 30 min to form homogeneous ink. Then, the ink was drop coating onto a CP (1 x 1 cm^2). The Pt/C/CP and RuO$_2$/CP electrodes were also prepared through the same procedure.
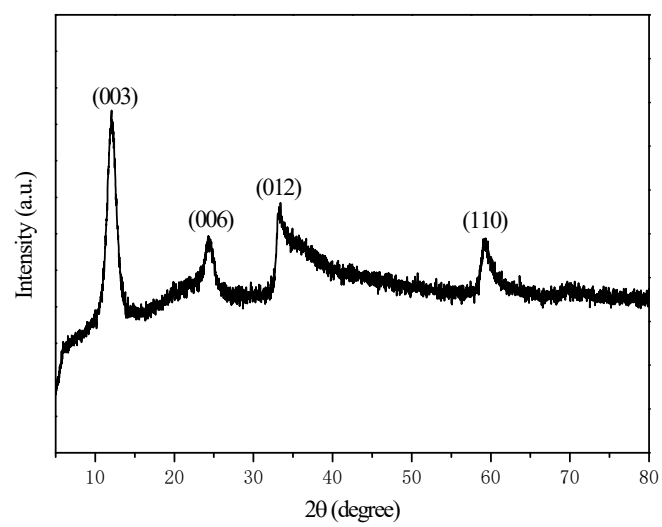
Figure S1. XRD pattern of Ru-Co LDH/Ti$_3$C$_2$T$_x$ MXene.
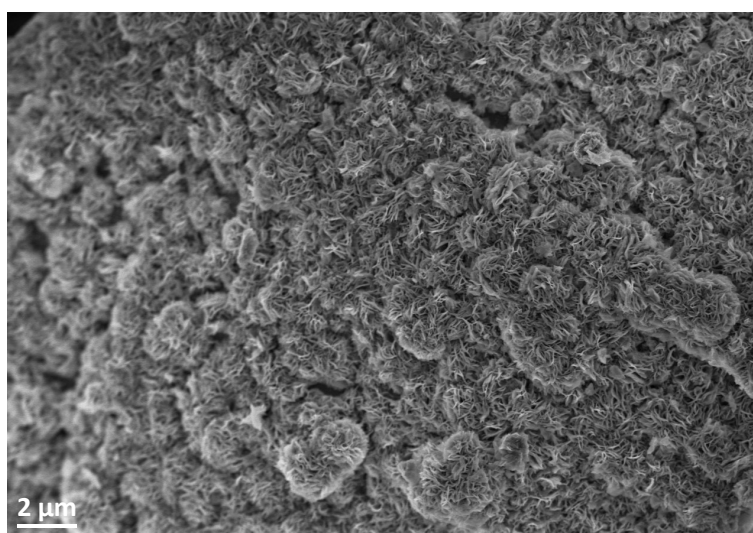

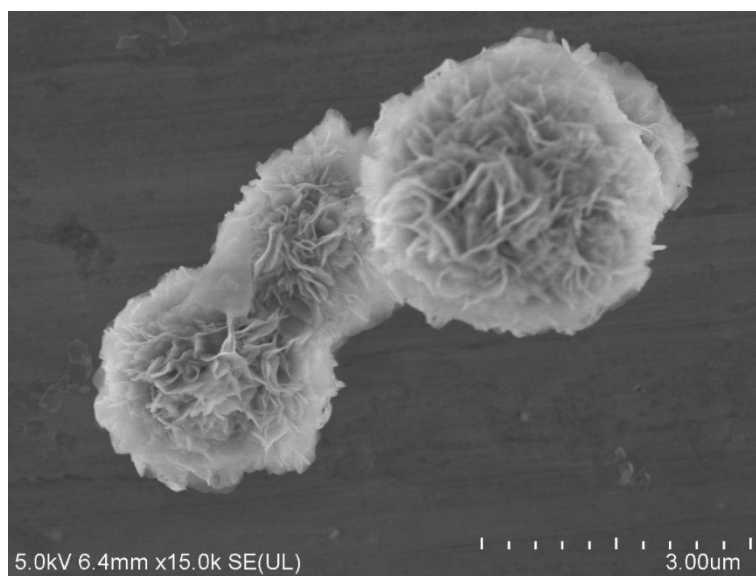**Figure S2.** SEM image of CoN/Ti$_3$C$_2$T$_x$ MXene.

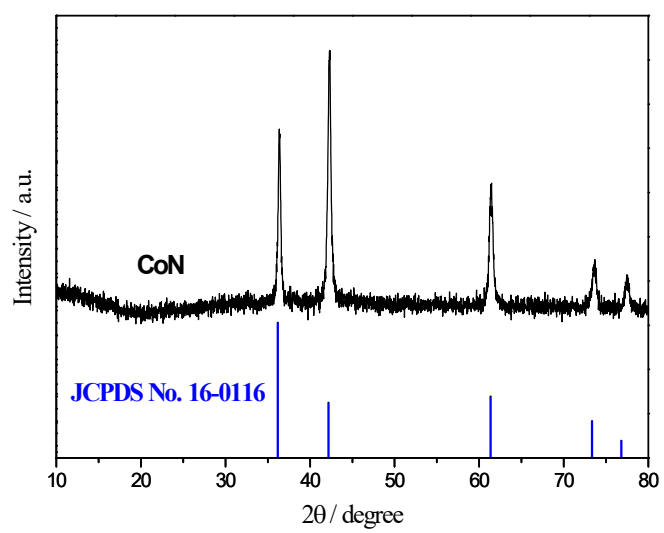**Figure S3.** SEM image of bare CoN.

Figure S4. XRD pattern of bare CoN.
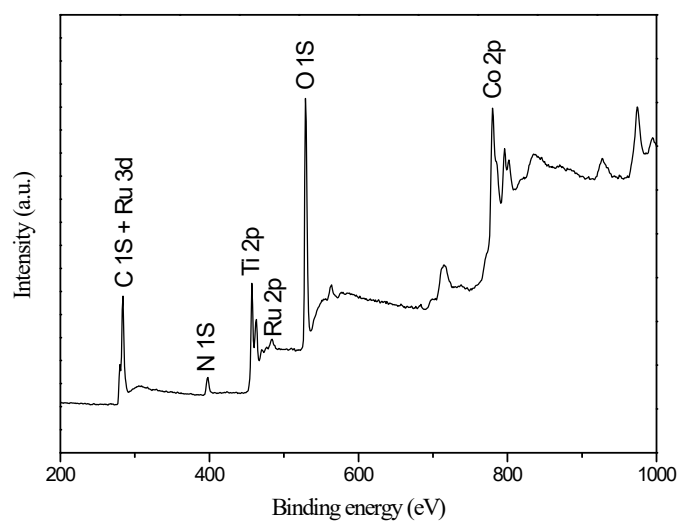
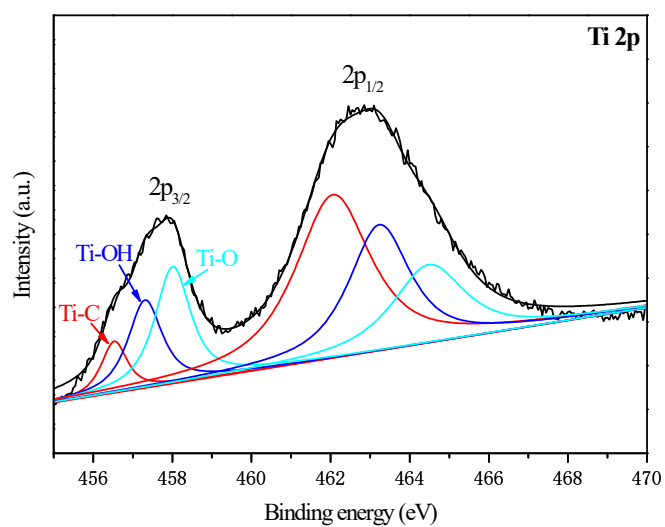**Figure S5**. Overall XPS spectra of Ru-CoN/Ti$_3$C$_2$T$_x$ MXene.

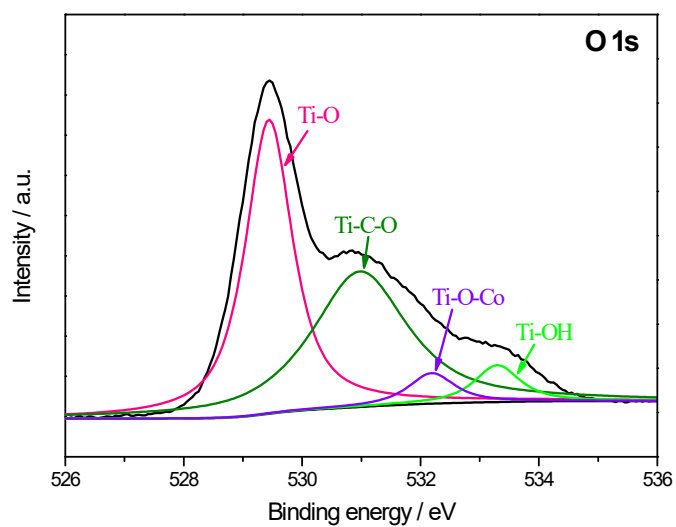**Figure S6**. High-resolution XPS spectra of Ti 2p for Ru-CoN/Ti$_3$C$_2$T$_x$ MXene.

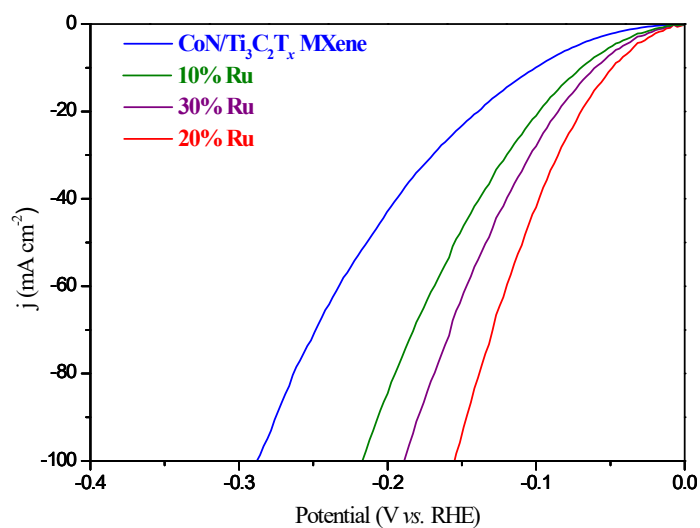**Figure S7.** High resolution XPS spectrum of O 1s for Ru-CoN/Ti$_3$C$_2$T$_x$ MXene.

Figure S8. HER polarization curves of the CoN/Ti$_3$C$_2$T$_x$ MXene with different Ru contents.
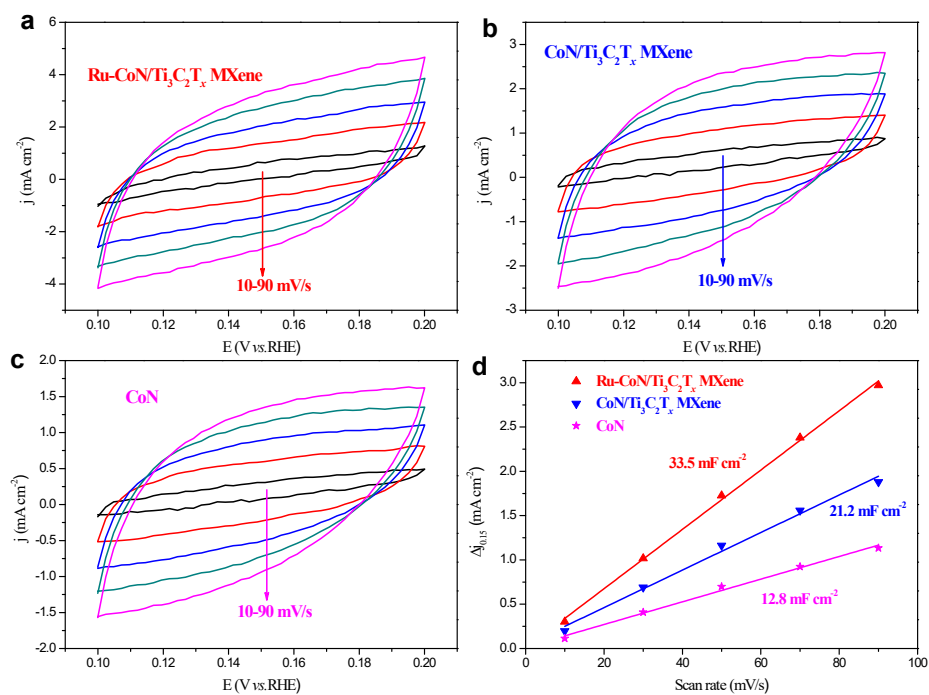
Figure S9. CV curves of (a) Ru-CoN/Ti$_3$C$_2$T$_x$ MXene, (b) CoN/Ti$_3$C$_2$T$_x$ MXene and (c) CoN with scan rates of 10, 30, 50, 70 and 90 mV s^{-1} in 1.0 M KOH. (d) Plots of the capacitive currents at 0.15 V as a function of scan rate for Ru-CoN/Ti$_3$C$_2$T$_x$ MXene, CoN/Ti$_3$C$_2$T$_x$ MXene, and CoN.
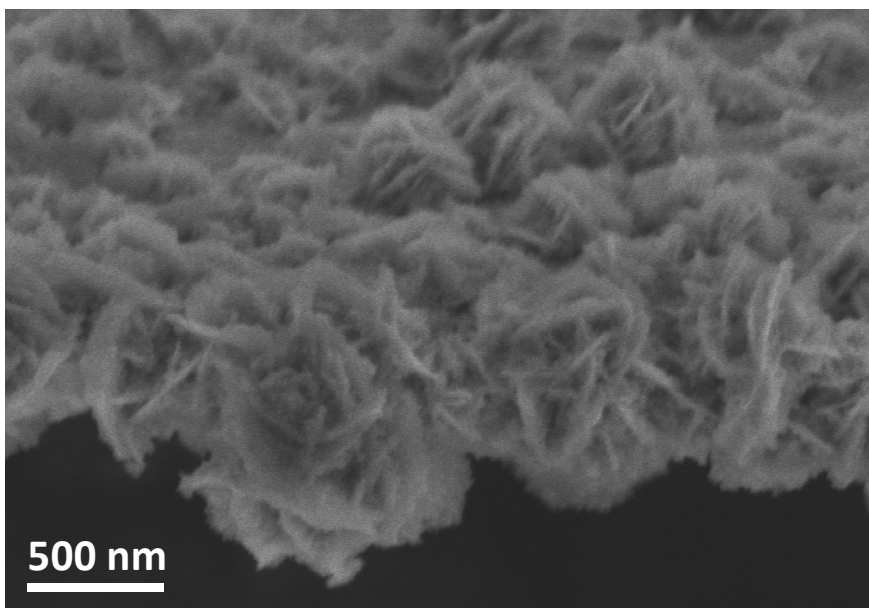
Figure S10. SEM image of Ru-CoN/Ti$_3$C$_2$T$_x$ MXene after HER test.
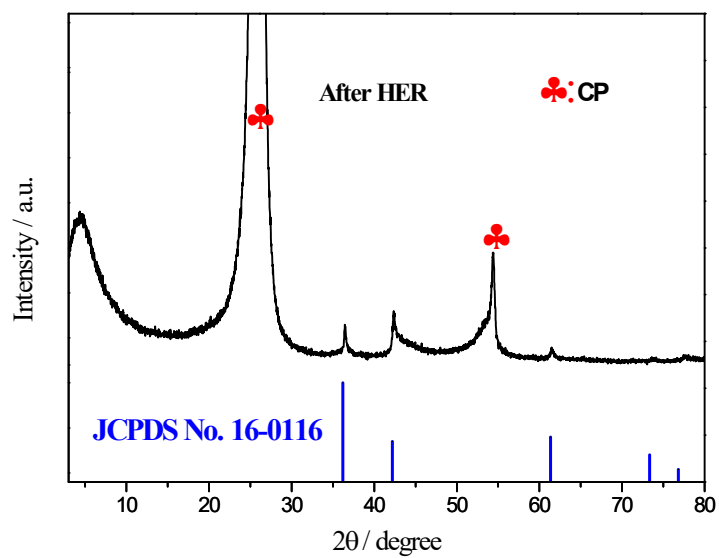
Figure S11. XRD pattern of Ru-CoN/Ti$_3$C$_2$T$_x$ MXene on CP after HER test.
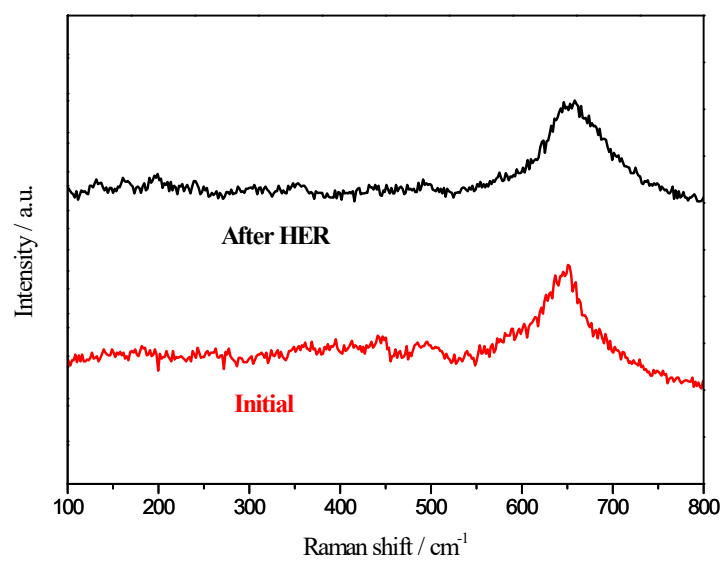
Figure S12. Raman spectra of Ru-CoN/Ti$_3$C$_2$T$_x$ MXene before and after HER test.
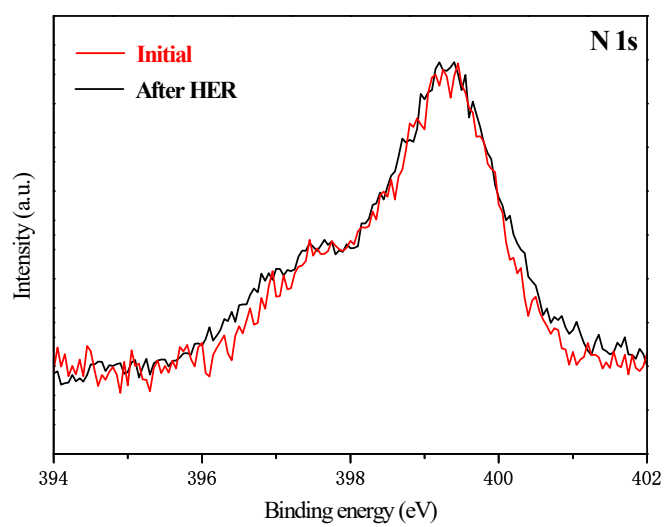

Figure S13. N 1s XPS spectra of Ru-CoN/Ti$_3$C$_2$T$_x$ MXene before and after HER test.
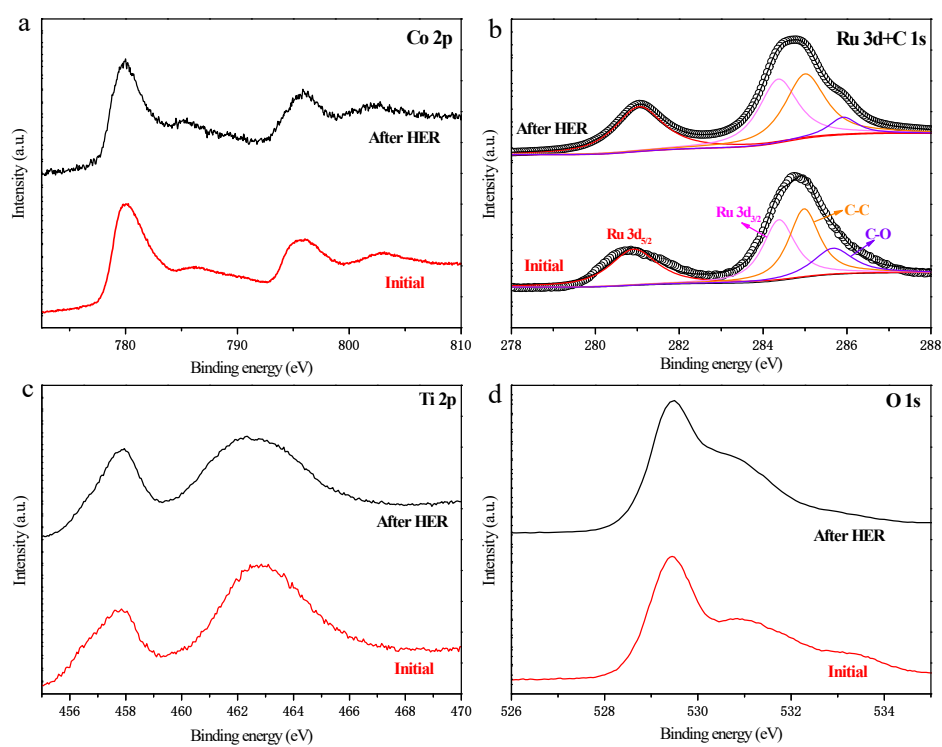
Figure S14. High-resolution XPS spectra of (a) Co 2p, (b) Ru 3d + C 1s, (c) Ti 2p, and (d) O 1s for Ru-CoN/Ti$_3$C$_2$T$_x$ MXene before and after HER test.
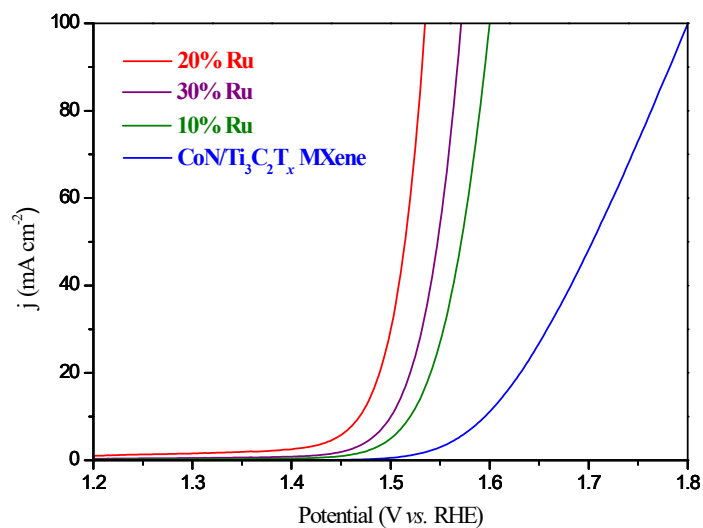
Figure S15. OER polarization curves of the CoN/Ti$_3$C$_2$T$_x$ MXene with different Ru contents.
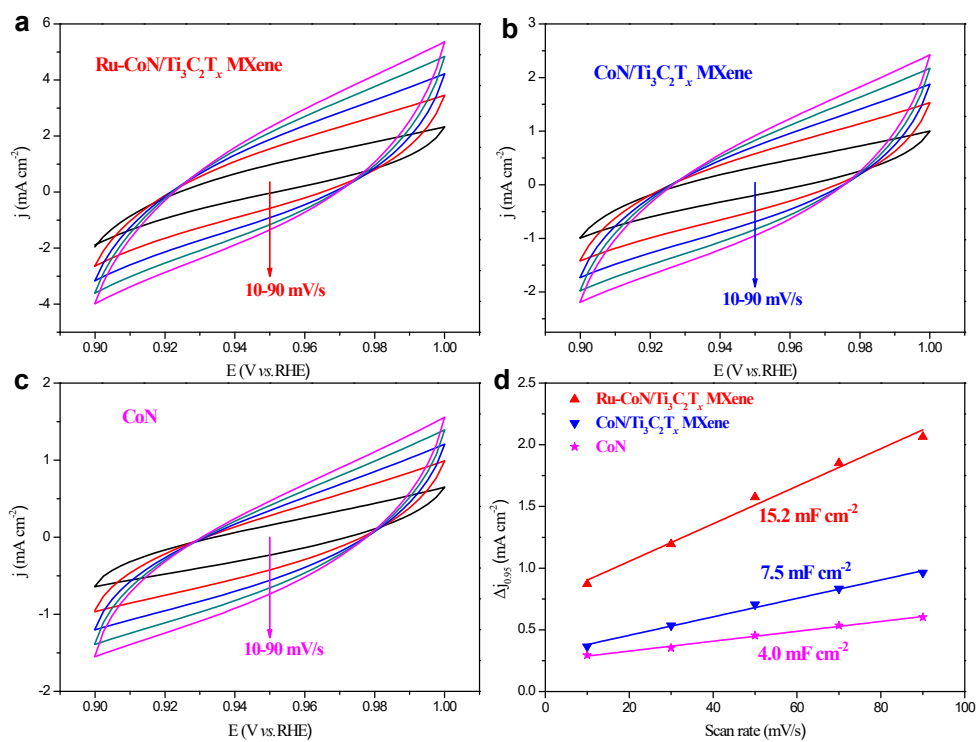
Figure S16. CV curves of (a) Ru-CoN/Ti$_3$C$_2$T$_x$ MXene, (b) CoN/Ti$_3$C$_2$T$_x$ MXene and (c) CoN with scan rates of 10, 30, 50, 70 and 90 mV s^{-1} in 1.0 M KOH. (d) Plots of the capacitive currents at 0.95 V as a function of scan rate for Ru-CoN/Ti$_3$C$_2$T$_x$ MXene, CoN/Ti$_3$C$_2$T$_x$ MXene and CoN.
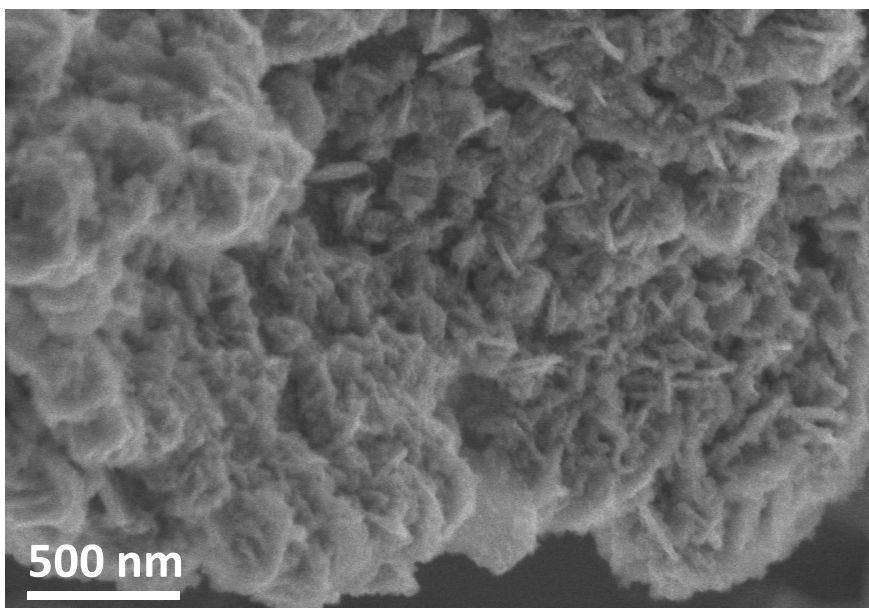
Figure S17. SEM image of Ru-CoN/Ti$_3$C$_2$T$_x$ MXene after OER test.
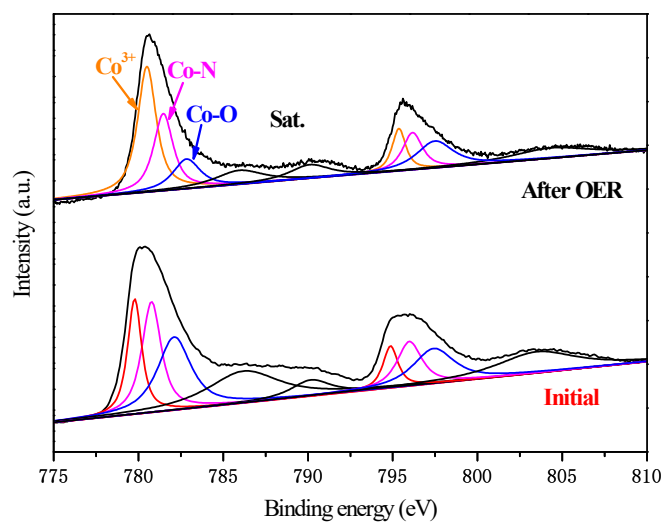
Figure S18. High resolution Co 2p XPS spectra of the Ru-CoN/Ti$_3$C$_2$T$_x$ MXene before

and after the OER test.

Figure S19. High resolution O 1s XPS spectra of Ru-CoN/Ti$_3$C$_2$T$_x$ MXene before and after OER test.

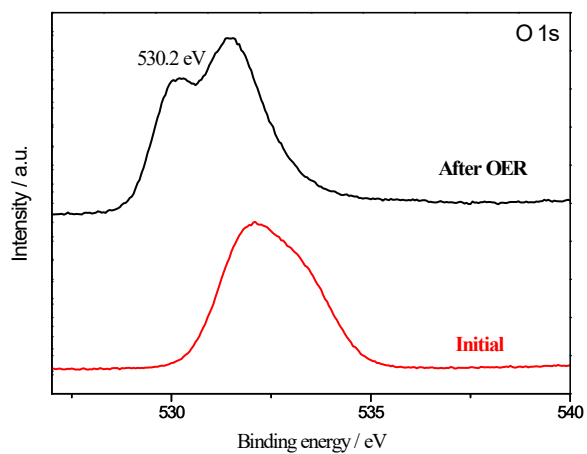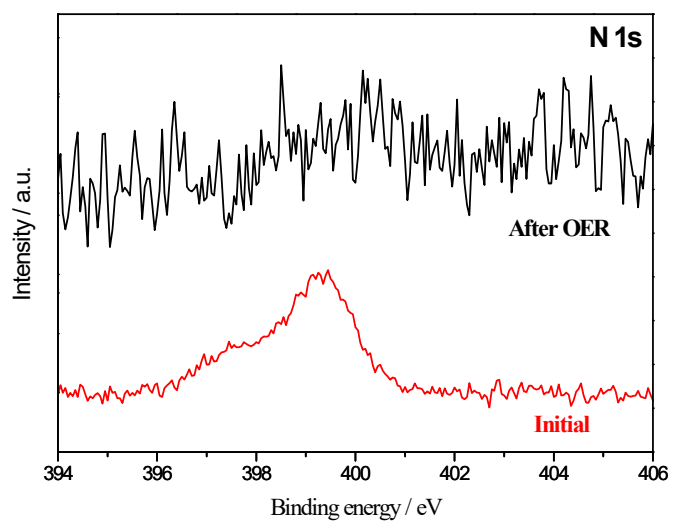**Figure S20**. High resolution N 1s XPS spectra of the Ru-CoN/Ti$_3$C$_2$T$_x$ MXene before and after the OER test.
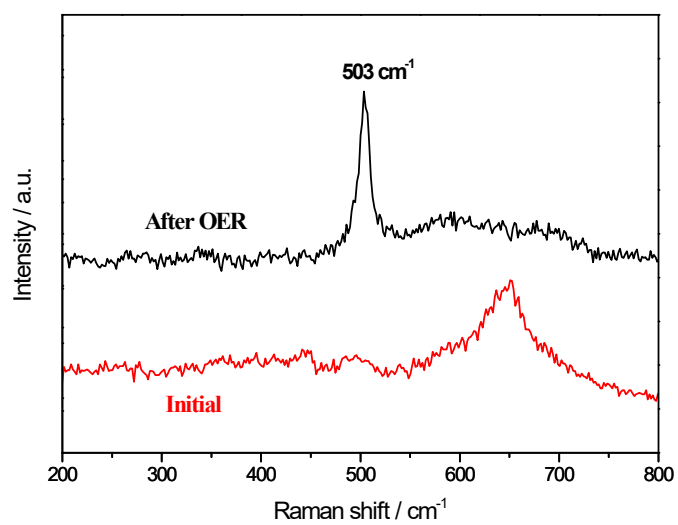
Figure S21. Raman spectra of the Ru-CoN/Ti$_3$C$_2$T$_x$ MXene before and after the OER test.
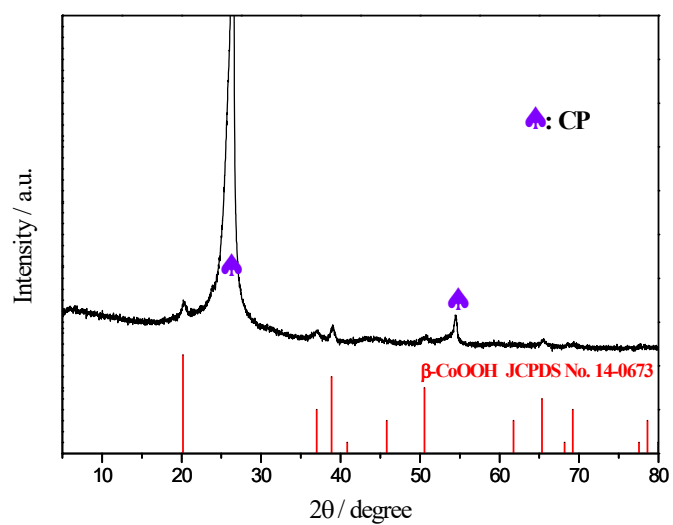

Figure S22. XRD pattern for Ru-CoN/Ti$_3$C$_2$T$_x$ MXene@CP electrode after the OER test.

Table S1. A comparison of HER performances of Ru-CoN/$Ti_3C_2T_x$ MXene with recently reported TMN-based electrocatalysts in 1.0 M KOH.

Catalyst	η (mV) at 10 mA cm^{-2}	Tafel slope mV dec^{-1}	Reference
Ni_3FeN-NPs	158	42	*Adv. Energy Mater.* **2016**, *6*, 1502585
NiMoN/CC	109	95	*Adv. Energy Mater.* **2016**, *6*, 1600221
NC@$CuCo_2N_x$/CF	105	76	*Adv. Funct. Mater.* **2017**, *27*, 1704169
Ni_3N/CMFs/Ni_3N	115	52.1	*J. Mater. Chem. A* **2017**, *5*, 9377
$Co_{5.47}N$ NP@N-PC	149	86	*ACS Appl. Mater. Interfaces* **2018**, *10*, 7134
Co-Ni_3N/CC	194	156	*Adv. Mater.* **2018**, *30*, 1705516
Ni_3FeN/r-GO	94	90	*ACS Nano* **2018**, *12*, 245
Co_3O_4-Co_4N PNSNs/HCC	90	57.8	*J. Mater. Chem. A* **2019**, *7*, 775
Ni_3N	133	103	*ACS Catal.* **2019**, *9*, 9332
h-MoN@BNCNT	118	59	*Adv. Funct. Mater.* **2019**, *29*, 1805893
Ni_3N/NF	120	110	*ACS Appl. Mater. Interfaces* **2019**, *11*,13168
NiCoN/C	103	NA	*Adv. Mater.* **2019**, *31*, 1805541
P,W-Co_3N NWA/NF	41	40	Nat. Commun. 2020, 11, 1853
P-Fe_3N@NC NSs/IF	102	68.59	*Small* **2020**, *16*, 2001980
Ru-Mo_2N	16	35	*Nano Energy* **2020**, *75,* 104981
P-MoP/Mo_2N	89	78	*Angew. Chem. Int. Ed.* **2021**, *60*, 6673
Ni_3N-V_2O_3@NF	57	50	*Appl. Catal. B: Environ.* **2021**,*286*, 119882
Ni_3N-Co_3N PNAs/NF	43	35.1	*Angew. Chem. Int. Ed.* **2021**, *60*, 5984
Ru-CoN/$Ti_3C_2T_x$ MXene	48.8	44.1	This work

Table S2. A comparison of OER performances of Ru-CoN/Ti$_3$C$_2$T$_x$ MXene with recently reported TMN-based electrocatalysts in 1.0 M KOH.

Catalyst	η (mV) at 10 mA cm^{-2}	Tafel slope mV dec^{-1}	Reference
Co$_4$N NW/CC	257	44	*Angew. Chem. Int. Ed.* **2015**, *54*, 14710
TiN@Ni$_3$N	350	93.7	*J. Mater. Chem. A* **2016**, *4*, 5713
Ni$_3$FeN-NPs	280	46	*Adv. Energy Mater.* **2016**, *6*, 1502585
FeCo-Co$_4$N/N-C	280	40	*Adv. Mater.* **2017**, *29*, 1704091
Ni$_3$N/CMFs/Ni$_3$N	273	41.54	*J. Mater. Chem. A* **2017**, *5*, 9377
Co$_{5.47}$N NP@N-PC	248	54	*ACS Appl. Mater. Interfaces* **2018**, *10*, 7134
Co-Ni$_3$N/CC	307	57	*Adv. Mater.* **2018**, *30*, 1705516
Mn$_3$N$_2$/NF	270	101	*Angew. Chem. Int. Ed.* **2018**, *57*, 698
Ni$_3$FeN/r-GO	270	54	*ACS Nano* **2018**, *12*, 245
Ni$_3$N-NiMoN/CC	277	118	*Nano Energy* **2018**, *44. 353*
Ni$_3$N/BP-AG	233	42	*Small* **2019**, *15*, 1901530
Ni$_2$Co-N	214	53	*Appl. Catal. B: Environ.* **2020**, *270, 118889*
NiFeMnN/Ti$_3$C$_2$ MXene	300	60	*Nano Lett.* **2020**, *20*, 2892
P-Fe$_3$N@NC NSs/IF	270	89.72	*Small* **2020**, *16*, 2001980
S-Ni$_3$FeN/NSG	260	76	*Appl. Catal. B: Environ.* **2020**, *274, 119086*
Co$_4$N-CeO$_2$/GP	239	37.1	*Adv. Funct. Mater.* **2020**, *30*, 1910596
Ni$_3$N/Ni@Ni$_3$N@CC	229	55	*Nano Energy* **2020**, *78, 105355*
2D CoNC@Co$_2$N HS	217	66	*Adv. Energy Mater.* **2020**, *10, 2002214*
Ru-CoN/Ti$_3$C$_2$T$_x$ MXene	238	68	This work

Table S3. Summary of recent reported representative of bifunctional TMN-based catalysts for overall water-splitting in 1.0 M KOH.

Catalyst	Potential (V) at 10 mA cm^{-2}	Reference
Fe$_2$Ni$_2$N/NF	1.65	*Inorg. Chem. Front.* **2016**, *3*, 630
TiN@Ni$_3$N	1.64	*J. Mater. Chem. A* **2016**, *4*, 5713
Ni$_3$N/CMFs/Ni$_3$N	1.59	*J. Mater. Chem. A*, **2017**, *5*, 9377
NiMoN	1.563	*J. Mater. Chem. A*, **2017**, *5*, 13648
CoN-Ni$_3$N/CC	1.56	*J. Mater. Chem. A*, **2018**, *6*, 4466
Ni$_3$FeN/r-GO	1.60	*ACS Nano* **2018**, *12*, 245
Co$_4$N-VN$_{1-x}$O$_x$@CC	1.64	*Appl. Catal. B: Environ.* **2019**, *241*, 521
FeOOH@Co$_4$N/SSM	1.59	*ACS Appl. Mater. Interfaces* **2019**, *11*, 5152
WN-Ni(OH)$_2$@CFP	1.705*	*ACS Catal.* **2020**, *10*, 13323
P-Fe$_3$N@NC NSs/IF	1.61	*Small* **2020**, *16*, 2001980
Co$_4$N@NC	1.561	*ACS Energy Lett.* **2020**, *5*, 692
FeOOH/Ni$_3$N	1.58	*Appl. Catal. B: Environ.* **2020**, *269*, 118600
Ni$_2$Co-N/CC	1.59	*Appl. Catal. B: Environ.* **2020**, *270, 118889*
SFCNF/Co$_{1-x}$S@CoN	1.58	*Small* **2020**, *16,* 2002432
2D CoNC@Co$_2$N HS-IN-CP	1.52	*Adv. Energy Mater.* **2020**, *10,* 2002214
Co/WN-600	1.51	*J. Mater. Chem. A*, **2020**, *8*, 22938
Co$_4$N-CeO$_2$/GP	1.507	*Adv. Funct. Mater.* **2020**, *30,* 1910596
Ru-CoN/Ti$_3$C$_2$T$_x$ MXene	1.52	This work

* Potential at 20 mA cm^{-2}